JJEE
Volume 11 | Number 2 | June 2025 | Pages 380-394

Jordan Journal of Electrical Engineering

ISSN (print): 2409-9600, ISSN (online): 2409-9619

Homepage: jjee.ttu.edu.jo

Exploring Leaky Feeder Cable as a Massive MIMO Solution for Next-Generation of 5G Networks

Hasan Farahneh[1*], Dia I. Abualnadi[2], Jamal S. Rahhal[3], Ibrahim Mansour[4]

[1, 2, 3] Electrical Engineering Department, School of Engineering, The University of Jordan, Amman, Jordan
E-mail: h.farahneh@ju.edu.jo

[4] Electrical Engineering Department, Faculty of Engineering Technology, Zarqa University, Zarqa, Jordan

Received: Jan 12, 2025 *Revised: Apr 13, 2025* *Accepted: Apr 24, 2025* *Available online: May 22, 2025*

***Abstract*—** Using a large number of individual antennas can significantly increase the costs associated with power consumption, as well as the hardware and software complexity of a massive MIMO system. In this paper, we present a relatively new approach and show how a hidden gem, which is the radiating cable or leaky feeder (LF) with large number of slot antennas can be configured to perform as a massive MIMO transceiver which satisfies the requirements of 5G networks, such as increasing coverage, ultralow latency, and data throughput. The LF MIMO systems will be significantly less complex and can work up to millimeter wave bands. Additionally, the LF can adapt its transmit power based on the number of slots with perfect channel state information (CSI) or the square root of the number of slots with insufficient CSI, aiming to achieve performance comparable to an equivalent single-input single-output (SISO) system. This paper provides a comprehensive analysis of the LF cable as a massive MIMO system, demonstrating its modeling as both point-to-point MIMO (P2P-MIMO) and a multi-user MIMO (MU-MIMO) system. Additionally, we evaluate key performance metrics, including bit error rate (BER), channel capacity, and energy efficiency. The findings indicate that the LF system performs effectively as a MIMO system. Notably, another significant result is that the received power of the LF in confined environments follows a **α-μ** distribution.

***Keywords*—** Leaky feeder; Massive MIMO; 5G; Energy efficiency; Spectral efficiency; α-μ distribution; Point-to-point system.

1. INTRODUCTION

Digital technological developments have made it possible for 5G mobile phone networks to offer high speed, high data rate, and low-latency communications. Nevertheless, the ability of these wireless services to satisfy this demand is limited. Existing usage of wireless connectivity to the Internet through smartphones, tablets, and PCs in buildings, structures like bridges, tunnels, and transportation systems like subways and highways are accommodated by the infrastructure of current wireless networks. But in order to accommodate more devices and/or faster data rates per device, 5G needs more infrastructure. Innovative and novel approaches are required to provide 5G services since the increased total costs per unit of capacity associated with this extra capacity are prohibitive [1].

Radiating or leaky coaxial cable which is shown in Fig. 1 is currently the most widely used antenna for locations that are challenging to cover traditional antennas. Underground mines, railroad and car tunnels, parking garages, hospitals, airports, office buildings, ships, offshore oil rigs, underground military installations, and airplanes are a few examples of such locations [2].

* Corresponding author
DOI: https://doi.org/10.5455/jjee.204-1736496553

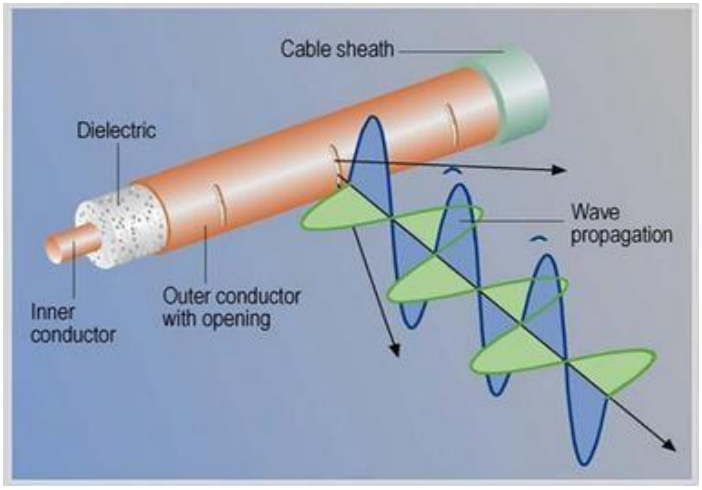

Fig. 1. Basic configuration of the leaky coaxial cable [15].

Despite its advantages such as: short range broadband wireless connectivity, ideal for micro and pico cells, and its characterization as a MIMO transceiver, an LF has been disregarded in before, but it has been taking it into consideration for a few years ago. Until now, it is anticipated that in future wireless communication systems with short air interfaces, the LF will be crucial [1]. The LF with precisely designed slots, functions as a bidirectional antenna array for signal transmission and reception, while also delivering DC power for amplifiers and active nodes. LF radio systems offer broad bandwidth, reduced noise, and compatibility with multiple RF transmissions [3]. Advanced low-loss cable types had been developed for optimal radiation and coupling. To ensure accuracy, the LF is best modeled as a linear antenna array, enabling its simulation as a large-scale MIMO system essential for 5G networks [3]. Conventional MIMO technology, widely adopted by wireless standards, enhances network capacity and reliability. However, standard MIMO implementations typically use fewer than 10 antennas at the base station, resulting in only modest improvements in spectral efficiency due to hardware complexity and cost, signal processing overhead**,** space constraints, channel correlation and energy consumption [4]**.** Massive MIMO systems, with base stations equipped with 100 or more antennas, have been introduced to simplify signal processing and deliver greater benefits. [5, 6]. Massive MIMO system is ideal for the large bandwidths and short-range radio cells of future wireless communications. However, practical implementation faces significant challenges due to the high hardware costs and complexity of wiring, matching circuits, amplifiers, filters, and RF units for each antenna. Additionally, the computational demands of signal processing algorithms for numerous antenna nodes add considerable software complexity. Much research has been conducted about LF. Authors in [7] proposed a novel method to selectively enhance the radiation performance of coupled mode leaky coaxial cables (LCX). By printing periodically spaced metallic stripes on the LCX's jacket, the design partially converts the bounded nonfoliar mode into a radiating mode, thereby improving radiation performance. Established a mathematical model for leaky coaxial cables, analyzing impedance and admittance to understand transmission attenuation characteristics had been introduced in [8]. Authors in [9] compared the signal strength between LFs cables and conventional Access Points, measurements indicated similar performance. However, while the signal is effectively distributed, there is a slight reduction in upload and download speeds due to signal attenuation along the cable. Despite this, test results meet Telecommunications and Internet Protocol Harmonization Over

Networks (TIPHON) standards, demonstrating the viability of LFs cables as a reliable medium for VoIP transmission.

Massive MIMO systems significantly increase power consumption. However, leveraging the LF as a large MIMO transceiver offers several advantages. It naturally functions as an antenna array with multiple radiating slots, avoiding additional costs or complexity. These slots can be engineered for beam forming to enable space division multiple access (SDMA), allowing multiple users to share bandwidth within a single cell. Additionally, the numerous antennas enhance channel stability and reduce outages caused by diversity [10].

An additional benefit of long wavelength (LF) is its strong support for millimeter bands, which are ideal for short-range communications systems in 5G networks. Furthermore, by employing simple linear signal processing methods as matched filter precoding and detection, an LF system can operate as a large MIMO system. The LF can be modeled as a linear antenna array, a one - dimensional configuration that transmits signals on a two-dimensional plane. The array's configuration, including antenna (slot) spacing and periodicity, significantly impacts communication performance, channel characteristics, and massive MIMO capacity. The fixed or adjustable slot periodicity can be optimized to enhance specific radiation properties [11, 12]. With its numerous slots, the LF is well-suited as a Multi-User MIMO (MU-MIMO) transceiver, offering greater resilience to propagation environment variations compared to single-user MIMO.

This makes the LF MU-MIMO technique applicable to various communication standards, including LTE, Wi-Fi (802.11), WiMAX (802.16), and 5G [13]. The LF can adjust it transmit power based on the number of slots with perfect or poor CSI to match the performance of a SISO system, resulting in significant energy savings [14]. This energy efficiency, enabled by its large number of slots, is crucial for future wireless networks where reducing energy consumption is increasingly important [15].

As any practical system, LF system has some limitations such as: LF systems experience signal loss along the cable length, necessitating the installation of line amplifiers at intervals to maintain signal strength.

This requirement increases both the complexity and cost of the system. Also, the deployment of LF cables demands precise installation to ensure consistent signal coverage. The harsh underground conditions can lead to physical damage of the cables, requiring regular maintenance and potential system downtimes [16].

In this paper, we present the LF as P2P transceiver and examine its performance in section 2. In Section 3, the LF's performance as MU-MIMO is examined. The spectral energy and energy efficiency are covered in Section 4. Section 5 shows the simulation and numerical results. In Section VI, conclusions are finally given.

2. MODELING THE LEAKY FEEDER AS A POINT-TO-POINT TRANSCEIVER

This section examines the benefits of modeling an LF as a P2P system from an information-theoretical perspective. First, we will consider the P2P-MIMO system. Assume that an LF is a P2P-MIMO transmission, with the transmitter has N broadcast slots (antennas) and the receiver has about K antennas.

In this work, a narrow-band, time-invariant channel with a deterministic and constant channel matrix $\mathbf{H} \in \mathbf{C}^{K \times N}$ are considered because we assume the LF in a short tunnel so we can neglect Doppler effect. To transform a frequency-selective wide-band channel into multiple

parallel narrow-band channels that experience flat fading, OFDM-based techniques are applied [17]. Let $\mathbf{x}$, and $\mathbf{y}$ be the transmitted signal vector and the received signal vector respectively, where $\mathbf{x} \in \mathbf{C}^{N\times 1}$ and $\mathbf{y} \in \mathbf{C}^{K\times 1}$ as shown in Eqs. (1) and (2), respectively.

$$\mathbf{x} = \begin{bmatrix} S_1(t) \\ S_2(t) \\ S_3(t) \\ \vdots \\ S_N(t) \end{bmatrix} \tag{1}$$

$$\mathbf{y} = \sqrt{\rho}\mathbf{H}\mathbf{x} + \boldsymbol{n_0} \tag{2}$$

where $\rho = \frac{A_T^2}{2}$ is the power of the LF is transmitted from all slots, A_T is the carrier's amplitude, and $\boldsymbol{n_0} \in \boldsymbol{C^{K\times 1}}$ is a noise vector.

Even though theoretical models assume normalized power levels, the total transmitted power in real-world communication systems is frequently subject to a variety of limitations that impact the possible data speeds. Power amplifiers utilized in transmission networks are one major drawback. Pushing these amplifiers above their limitations results in non-linearities and signal distortion, which lower the overall signal quality. These amplifiers have limited power-handling capabilities. The maximum signal intensity that can be broadcast is therefore limited since the transmitted power must be maintained within safe operating limits to guarantee signal integrity. The real signal intensity at the receiver is frequently less than predicted by theoretical models that normalize total transmitted power because of these practical limitations. The Signal-to-Noise Ratio (SNR) is directly impacted by this signal strength decrease, which lowers the possible data speeds. Because they do not take into consideration these actual power constraints, the capacity expressions obtained under idealized assumptions may therefore overestimate the actual data rates. This emphasizes how crucial it is to take regulatory limitations and amplification constraints into account when developing and assessing communication systems in order to guarantee accurate performance evaluations [18].

Assuming that the total power of the transmitted signal is normalized i.e., $E\ \|X^2\| = 1$, and the noise has zero mean with identity covariance matrix I. Because it simplifies computations, theoretical analysis usually assumes independent, identically distributed (i.i.d.) noise with unit variance. This is especially true when applying techniques like Maximum Likelihood Estimation or when calculating performance metrics like (SNR). The Rayleigh fading assumption is also accurate in many real-world scenarios, particularly when the transmitter and receiver are not in line of sight and the received signal is the result of many reflections or scattering from surrounding objects. When there are several scatterers, the resulting channel can be simulated using a Rayleigh distribution. This is particularly true in metropolitan environments where many objects scatter and cause diffraction [19].

Since Quadrature Phase Shift Keying (QPSK) is widely used in many applications where an ideal trade-off between spectral efficiency, power efficiency, and resilience is required because of its benefits, which include power efficiency, spectral efficiency, and robustness against noise in 5G applications. Here, we will use QPSK., the transmitted signal from an arbitrary slot is given as [20]:

$$S_n(t) = Ae^{j\omega_c t} e^{\frac{j(2m-1)\pi}{4}} 10^{\frac{-znr}{20}} e^{\frac{j2\pi znv}{\lambda}} \tag{3}$$

where $\omega_{c\ (rad/sec)}$ is the carrier frequency, $z\ in\ (m)$ is the distance between the slots, n is the slot index, v is the relative phase velocity (m/s), r is the cable attenuation (dB\km), and $\lambda\ (m)$ is the wavelength.

The combined signal from all slots will be represented by the real part of Eq. (4).

$$S(t)_T = Re\left[\sum_{n=1}^{N} Ae^{j\omega_c t} e^{\frac{j(2m-1)\pi}{4}} 10^{\frac{-znr}{20}} e^{\frac{j2\pi znv}{\lambda}}\right] \quad (4)$$

where m is number of constellations (m = 4) in QPSK modulation. The new amplitude (AT) of all signals from all slots will then be:

$$A_T = \sqrt{\left(\begin{array}{c}\left(\sum_{n=1}^{N} A10^{\frac{-znr}{20}} cos\left(\frac{(2m-1)\pi}{4} + \frac{2\pi znv}{\lambda}\right)\right)^2 + \\ \left(\sum_{n=1}^{N} A10^{\frac{-znr}{20}} sin\left(\frac{(2m-1)\pi}{4} + \frac{2\pi znv}{\lambda}\right)\right)^2\end{array}\right)} \quad (5)$$

The bit energy of the received signal is expressed as:

$$E_b = \frac{A_T^2 T_b}{2} \quad (6)$$

where T_b is the bit duration, A is the amplitude of the bit.

Assuming independent and identically distributed (*i.i.d*) transmitted signal and perfect CSI, the capacity of channel C will be:

$$C = log_2|\mathbf{I} + \bar{\gamma}_t| \quad (7)$$

where $\bar{\gamma}_t$ is the average SNR and it is given by [3].

$$\bar{\gamma}_t = \sum_{l=1}^{L} \left\{\left(\begin{array}{c}\left(\sum_{n=1}^{N} A10^{\frac{-znr}{20}} cos\left(\frac{(2m-1)\pi}{4} + \frac{2\pi znv}{\lambda}\right)\right)^2 + \\ \left(\sum_{n=1}^{N} A10^{\frac{-znr}{20}} sin\left(\frac{(2m-1)\pi}{4} + \frac{2\pi znv}{\lambda}\right)\right)^2\end{array}\right)\right\} \left\{\frac{T_b E[\alpha_l^2]}{N_0}\right\} \quad (8)$$

where $\boldsymbol{\alpha}$ is the path loss exponent. In the case of the LF system with high carrier frequency and small slot period $z = \frac{\lambda}{2}$, which means the number of slots will be very high ($N \to \infty$), the capacity can be written as

$$C = K\ log_2(1 + \rho) \quad (9)$$

It's good to mention here that theoretical analysis and mathematical derivations are greatly simplified by the assumption of perfect Channel State Information (CSI), the difficulties of practical implementations are not adequately captured. In real-world applications, quantization, feedback delays, and noise-induced CSI estimation mistakes can impair system performance, resulting in greater bit error rates (BER) and decreased capacity. When compared to real deployments, this disparity could make the results unduly optimistic. It would be advantageous to take into consideration models that take into account imperfect CSI, such as adding estimate errors or feedback delay effects, in order to increase the analysis's dependability and give a more realistic depiction of system performance under real-world circumstances [21].

The capacity of an LF system was previously calculated for QPSK modulation in a Rayleigh channel with no interference and a comparison with a single antenna was done, which showed an acceptable value of channel capacity of the LF. The BER of the LF in a Rayleigh fading channel was derived in [3] and is given as:

$$P_b(E) = I_1 I_2 \quad (10)$$

$$I_1 = \left(0.5 - 0.5\sqrt{\left(\frac{\bar{\gamma}_t}{1+\bar{\gamma}_t}\right)}\right)^L \quad (11)$$

$$I_2 = \sum_{l=1}^{L} \binom{L+l-1}{l} \left(0.5 - 0.5\sqrt{\left(\frac{\bar{\gamma}_t}{1+\bar{\gamma}_t}\right)}\right)^L \quad (12)$$

where l is the path index, and L is the total number of paths.

3. LEAKY FEEDER AS A MULTI USER TRANSCEIVER

We first need to look at the basic architecture, distinctions, and integration potential of Point-to-Point (P2P) and Multi-User MIMO (MU-MIMO) systems in order to comprehend how they connect.

MU-MIMO has a higher gain than P2P-MIMO system, since it cancels the undesired propagation environments effects. To model the LF as a MU-MIMO, we consider a LF with N slots that serve K single users with one receiving antenna for each, where ($N >> K$), also, considering OFDM with M subcarrier. Assuming the bandwidth of the symbol does not significantly exceed the channel's coherence bandwidth at each subcarrier (flat fading) and the LF has perfect CSI,

From the k^{th} user to the n^{th} slot, the channel coefficient will be:

$$h_{k,n} = g_{k,n}\sqrt{\beta_k} \quad (13)$$

where $g_{k,n}$ is a complex small-scale fading factor, and β is a large scaling coefficient, β is given by:

$$\beta_k = \phi d_k^{-\alpha} \xi_k \quad (14)$$

where ϕ is a constant associated with the carrier frequency and antenna gain. d_k is the distance between the slot in the LF and the k^{th} receiver, and ξ_k is the log normal shadow fading with $\xi_k \sim N(0,\sigma^2_{sh})$. It is good to mention that it is possible to use log-normal shadowing in tunnels, particularly when taking into account long-range signal fluctuations brought on by irregularities in the tunnel.

In this context, the small-scale fading coefficients vary across different users or LF slots, while the large-scale fading coefficients are assumed to be consistent across slots but vary depending on the user.

The channel matrix for all users to the LF is represented as:

$$\mathbf{H}_k = \mathbf{G}\mathbf{D}^{\frac{1}{2}} \quad (15)$$

where the three matrices **H**, **G** and **D** are given by:

$$\mathbf{H} = \begin{bmatrix} h_{1,1} & h_{1,2} & \dots & h_{1,K} \\ h_{2,1} & h_{2,2} & \dots & h_{2.K} \\ \vdots & \vdots & \ddots & \vdots \\ h_{N,1} & h_{N,2} & \dots & h_{N,K} \end{bmatrix} \quad (16)$$

$$\mathbf{G} = \begin{bmatrix} g_{1,1} & g_{1,2} & \dots & g_{1,K} \\ g_{2,1} & g_{2,2} & \dots & g_{2.K} \\ \vdots & \vdots & \ddots & \vdots \\ g_{N,1} & g_{N,2} & \dots & g_{N,K} \end{bmatrix} \quad (17)$$

$$\mathbf{D} = diag\{\beta_1, \beta_2, \dots, \beta_K\} \quad (18)$$

$$\mathbf{D} = \begin{bmatrix} \beta_1 & 0 & \dots & 0 \\ 0 & \beta_2 & \dots & 0 \\ \vdots & \vdots & \ddots & \vdots \\ 0 & 0 & \dots & \beta_K \end{bmatrix} \quad (19)$$

3.1. Uplink

For uplink transmission process, the received signal vector $\mathbf{y_{up}} \in \mathbf{C}^{N\times 1}$ will have an expression as:

$$y_{up} = \sqrt{\rho_{up}}\mathbf{H}\mathbf{X}_{up} + \mathbf{n}_{up} \tag{20}$$

where ρ_{up} is the uplink transmitted power, $\mathbf{X_{up}} \in \mathbf{C}^{K\times 1}$ is the signal vector from all users, for example the transmitted symbol from the k^{th} user is determined as x_k^u which has the k^{th} order in $\mathbf{X_{up}}$, $\mathbf{n_{up}} \in \mathbf{C}^{N\times 1}$ is a complex Gaussian noise, $\mathbf{H} \in \mathbf{C}^{N\times K}$ is the channel matrix of the uplink. The vector $\mathbf{X_{up}}$ is given by

$$\mathbf{X}_{up} = \begin{bmatrix} x_1^u \\ x_2^u \\ \vdots \\ x_K^u \end{bmatrix} \tag{21}$$

As the number of slots increases, the column channel vectors from each user are asymptotically orthogonal. Assuming that the small-scale fading coefficients for each user are independent, $\mathbf{H}$ is decomposed as described in [22] as:

$$\mathbf{H^H H} = \mathbf{D}^{\frac{1}{2}}\mathbf{G^H G D}^{\frac{1}{2}} = N\mathbf{D}^{\frac{1}{2}}\mathbf{I}_K\mathbf{D}^{\frac{1}{2}} = N\mathbf{D} \tag{22}$$

$$C = log_2\left|\mathbf{I} + \rho_{up}\mathbf{H^H H}\right| \tag{23}$$

$$= log_2\left|\mathbf{I} + \rho_{up}N\mathbf{D}\right|$$

$$= \sum_{k=1}^{K} log_2\left|\mathbf{I} + \rho_{up}N\mathbf{D}\right| \qquad bps/Hz$$

In this work, we use the matched filter (MF) technique because it offers the best possible trade-off between resilience, complexity, power efficiency, and performance, MF is recommended in LF systems. The most practical and effective option for real-world applications is MF, which takes advantage of the distributed nature of LF, even though ZF and MMSE might perform better in centralized MIMO systems with a lot of interference [23, 24]. When the simple MF process is used with LF, same capacity can be obtained as in Eq. (23). The LF processes the signal vector by multiplying it with the conjugate transpose of the channel matrix, as follows:

$$\mathbf{H^H} y_{up} = \mathbf{H^H}(\sqrt{\rho_{up}}\mathbf{H}\mathbf{X}_{up} + \mathbf{n}_{up}) \tag{24}$$

$$= N\sqrt{\rho_{up}}\mathbf{D}\mathbf{X}_{up} + \mathbf{H}\mathbf{n}_{up}$$

From Eq. (23), the SNR for the k^{th} user is given as:

$$SNR = N\rho_{up}d_k \tag{25}$$

When the number of slots increases to infinity, simple matched filter processing with the LF is ideal since the channel capacity when using a matched filter is equal to the limit in (23) as well.

3.2. Downlink

In the downlink case a time-division duplexing (TDD) mode is used. The received signal vector $\mathbf{y_d}$ is given by:

$$\mathbf{y}_d = \sqrt{\rho_d}\mathbf{H}\mathbf{X}_d + \mathbf{n}_d \tag{26}$$

where X_d, ρ_d and n_d are the transmitted signal vector, the transmitted power and the noise of the downlink respectively. Authors in [25] showed that, the base station-LF can allocate power in a way that maximizes the total transmission rate. The capacity can be determined by

decomposing the vector channel into a series of independent, parallel scalar Gaussian sub-channels. The channel capacity measured in bps/Hz can be written as:

$$C = max_p\ log_2\left|\mathbf{I}_N + \rho_d \mathbf{HPH^H}\right| = max_p\ log_2|\mathbf{I}_K + \rho_d N\mathbf{PD}| \quad (27)$$

$$\rho_d = \sum_{n=1}^{N} A10^{\frac{-znr}{20}}\cos(\frac{2\pi znv}{\lambda}) \quad (28)$$

And **P** is a diagonal positive matrix that determines the power allocation where the sum of its diagonal elements =1. Assuming the matched filter Precoder is used, the transmitted signal vector is:

$$\mathbf{X}_d = \mathbf{H}^*\mathbf{D}^{\frac{-1}{2}}\mathbf{P}^{\frac{1}{2}}\mathbf{s}_d \quad (29)$$

where $\mathbf{s_d} \in \mathbf{C}^{K\times 1}$ is the source information vector. Additionally, when the number of slots reaches infinite, the received signal vector from every user becomes:

$$\mathbf{y}_d = \sqrt{\rho_d}N\mathbf{D}^{\frac{1}{2}}\mathbf{P}^{\frac{1}{2}}\mathbf{s}_d + \mathbf{n}_d \quad (30)$$

Because **D** and **P** are diagonal matrices, the signal transmission from the LF to each user can be considered as SISO transmission, in this case the inter-user interference can be canceled. Furthermore, the data obtained can be maximized depending on matrix **P** i.e. the choices of power allocation.

4. ENERGY-EFFICIENCY OF THE LEAKY FEEDER SYSTEM

The increasing demand for high-data-rate applications necessitates higher energy consumption in wireless networks to improve communication system quality due to the rapid reproduction of high-data-rate applications. Moreover, the requirement for Eco-friendly transmission methods, communication networks' energy efficiency is becoming increasingly important.

Over the last decade, energy efficiency has been studied from an information-theoretic standpoint and many scenarios have been suggested [26]. The channel bit rate R for the LF system with a Gaussian channel and total transmit power ρ and system B is determined by:

$$R = \frac{1}{2}log_2\left(1 + \frac{\rho}{N_0 B}\right) \quad (31)$$

Bits per real dimension or degrees of freedom. The Nyquist sampling theory states that there are $2B$ degrees of freedom each second. The channel capacity is therefore $C = 2BR$ b/s. As a result, the energy efficiency η_{EE} is given as:

$$\eta_{EE} = \frac{C}{\rho} = \frac{2R}{N_0(2^{2R}-1)} \quad (32)$$

Theoretical energy efficiency values may not be realized in a real system due to a variety of reasons, including capacity-approaching, channel code performance loss, CSI knowledge gaps [27], synchronization cost [28], and energy consumption associated with transmission - related electronic circuits.

The basic trade-off between energy efficiency and data rate is altered for all of these aspects by the energy consumption of electronic circuits. Energy efficiency must be redefined as information bits per unit of energy, taking into account circuit energy consumption and adding an extra circuit power factor P_c [29].

$$\eta_{EE} = \frac{C}{\rho} = \frac{2R}{N_0 P_c(2^{2R}-1)} \quad (33)$$

The power consumption in the LF system will be less than conventional MIMO system because LF needs less complexity of the hardware circuits, so our view of conventional energy saving techniques may change [29]. More studies should be done to compare the match filter precoder with zero-forcing pre-coder of the LF system to show which one can do better in terms of energy efficiency and spectrum.

5. SIMULATION AND NUMERICAL RESULTS

MATLAB software R2020b [30] was used for simulation in order to confirm the LF system's functionality and suitability for 5G by studying its performance. Perfect phase matching between the transmitter and the receiver with fading channels, and QPSK modulation have all been taken into consideration. Also, in our simulation we consider moving objects in tunnels such as vehicles. For those moving objects we consider the velocity, Doppler shift effects, the Line-of-Sight channel gain and the Non line of sight gain as well. Table 1 shows the fixed parameters that were used in the simulation. Each figure displays the values of the variable parameters as appropriate, including the carrier frequency f (i.e., λ) and the slot period D.

Table 1. Parameters utilized in the simulation.

Parameter	Value
Bandwidth	10 MHz
Amplitude of the Carrier A	12 V
Carrier frequency	3 GHz
Phase velocity β	1 rad/s
Number of considering Paths L	3
Power of the noise N_0	0 dB
Axial attenuation k	0.17 dB/Km
Bit Duration T_b	0.1 ms
LF length	100 m

Fig. 2 shows how the leaky feeder system's capacity increases as the number of slots increases. The capacity has a non-linear relationship with the number of slots, growing rapidly at first before plateauing or tapering off based on system limitations.

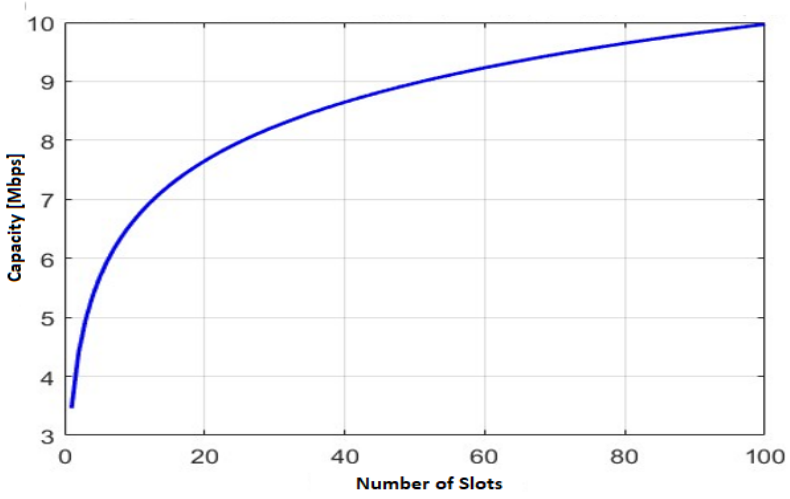

Fig. 2. Channel capacity with number of LF slots.

This pattern demonstrates how slots separation affects LF system performance optimization and the possible trade-offs between capacity expansion and signal quality or system efficiency. Also, we can note here that after a certain number of slots the capacity becomes almost fixed.

Moreover, Fig. 3 illustrates the relationship between energy efficiency and the number of slots in the LF system. Initially, energy efficiency shows a significant increase as the number of slots grows. The appropriate explanation for this behavior is due to many reasons such as: the additional slots introduce more power consumption without a proportional gain in performance. This could be due to increased interference, signal processing overhead, or diminishing returns in spatial diversity. However, the efficiency gain begins to diminish at higher slot counts, reflecting a saturation effect or diminishing returns. This trend suggests that there is an optimal range of slot numbers for maximizing energy efficiency, beyond which additional slots contribute less significantly to overall efficiency. Such insights are crucial for optimizing the design and operation of the LF system, balancing performance and energy consumption.

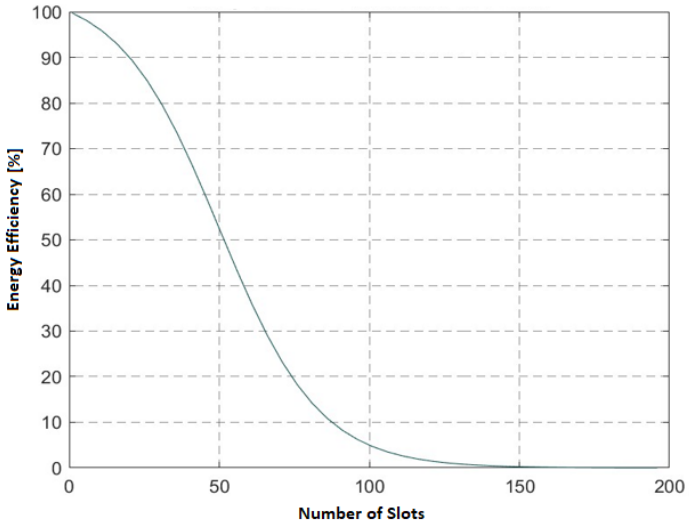

Fig. 3. Energy efficiency with number of LF slots.

Fig. 4 and Fig. 5 show a crucial result. It can be seen that, as the distance increases, the system BER performance decreases which is logic.

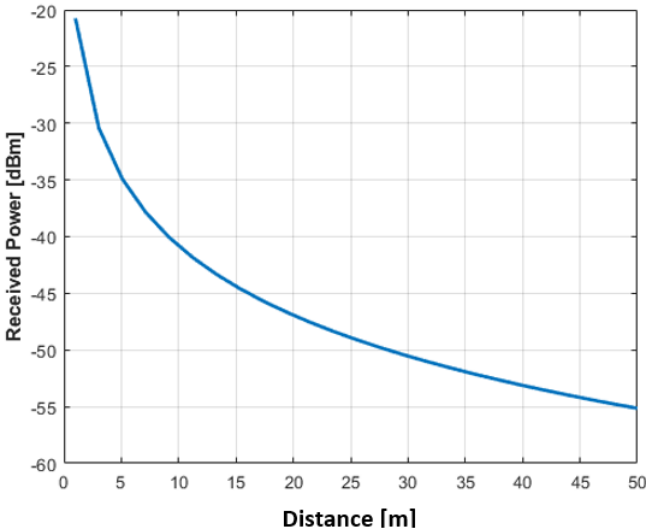

Fig. 4. Received power of LF vs the distance between the LF and the receiver.

Also, we can see from Fig. 4 and Fig.5 that, the value of the BER degrades from 10^{-5} at (distance = 1 m) to 3.5×10^{-2} at distance = 5 m. This happens because when the distance changes from 1 to 5 m, the received power reduces by more than 3 times (e.g., it decreases from -20 dBm to -35 dBm). Also, Fig. 4 and Fig. 5 show that at far distance > 20 m the BER becomes fixed because the transmitted energy becomes very low. Also, Fig. 5 shows that the BER almost fixed (saturated) as the distance between the LF and the receiver increases the saturation in the BER can be attributed to several factors. First, the energy of the received signal from a distant LF is weak, as its intensity is inversely proportional to the square of the distance between the LF and receiver. Another reason is that as the signal travels a longer distance, it may encounter multiple obstacles and interference from other signals, leading to further weakening.

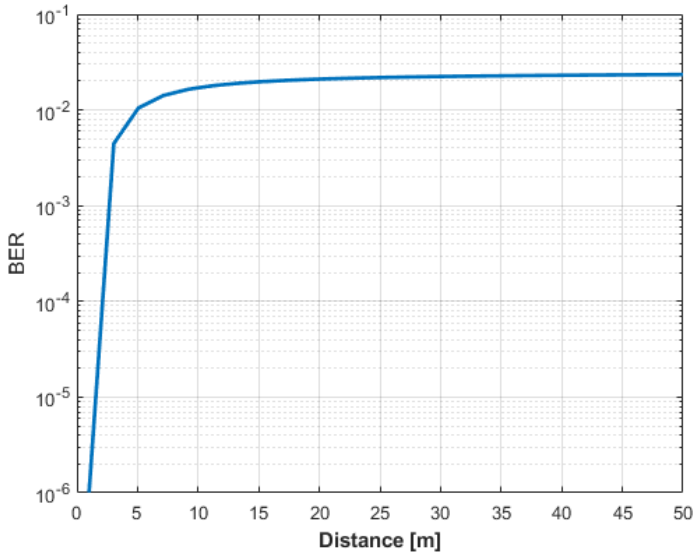

Fig. 5. BER of LF vs the distance between the LF and the receiver.

In Fig. 6, the carrier frequency employed is 3 GHz. Due to the phase-rotating characteristics of the LF, it is evident that the BER varies periodically. The periodic nature of the LF, multipath interference, standing wave effects, and phase shifts between slots are the main causes of the oscillatory behavior seen in the BER vs slot period plot. In order to minimize performance degradation in real-world LF deployments, it is essential to comprehend this behavior in order to design more effective modulation schemes and error correction approaches. A slot period of 20 mm results in the lowest BER. This is most likely the ideal value for the specified frequency. Keep in mind, nevertheless, that the slot separation must be practically possible for a specific LF cable (depending on its length, loss required, and other considerations). Too little separation will result in too much energy being radiated, and vice versa, since the ratio of transmitted to conducted RF energy is dependent on the slot period. High slot spacing causes the receiver to receive less energy, which is why there is a general pattern of the BER increasing as the slot period increases. This is most likely due to the fact that there are less (radiating) slots in a given length (100 m). Essentially, this figure demonstrates that a very low BER can be obtained by suitably adjusting an LF's slot time for a specific carrier frequency.

Fig. 7 illustrates the PDF of the received power; we made a curve fitting for the simulated data which closely resembles an $a-\mu$ distribution with a = 2 and μ = 2. This alignment suggests that the propagation environment is well-modeled by the $a-\mu$ framework, capturing the

small-scale fading characteristics of the LF system. This distribution looks suitable for LF system in confined areas, where this result aligns with previous works as [31].

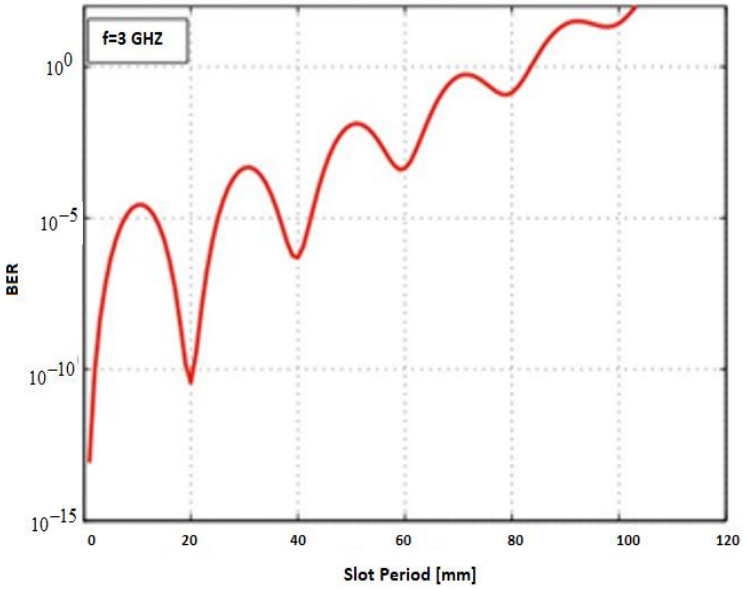

Fig. 6. Bit error rate vs. number of slots of the LF.

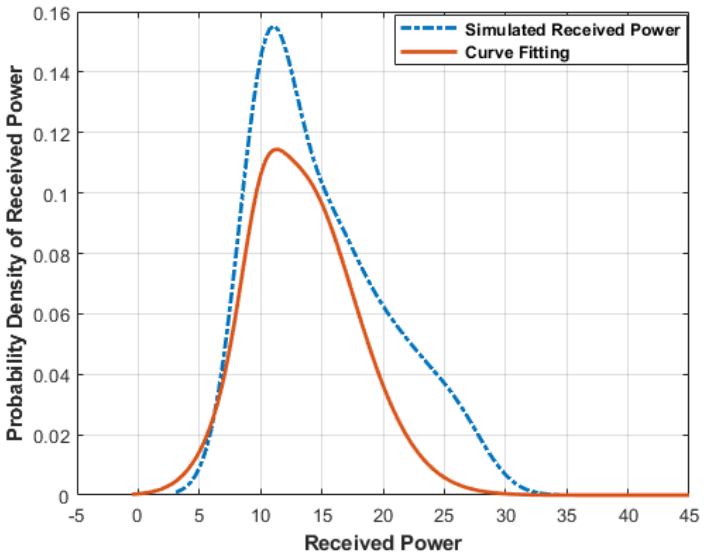

Fig. 7. PDF of the received power.

6. COMPARATIVE ANALYSIS

Finally, the majority of previous works discussed many issues about LFs and massive MIMO systems, but this work is unique in that it provides a comprehensive analysis of the Leaky Feeder (LF) cable as a massive MIMO system. The performance of LF cables in confined spaces, such as tunnels or subterranean facilities, has historically been the main focus of studies on the subject, with a particular emphasis on channel modeling, path loss, and coverage characteristics [32, 33].

Few of these studies have looked at LF systems' potential as scalable MIMO platforms, particularly when considering enormous MIMO. By including the LF structure into the massive MIMO framework, this article goes one step further and provides dual modeling capabilities for both P2P-MIMO and MU-MIMO systems. This study captures multi-user

dynamics, which makes it more applicable to developing 5G and beyond-5G network topologies than most previous works, which focus on simplified models or single-user systems.

Furthermore, compared to the widely used log-normal or Rayleigh distributions, which frequently fall short in capturing the composite fading and shadowing effects seen in underground or enclosed environments, the α-μ distribution offers a more realistic statistical model for describing the received power in confined environments. The analytical importance of α-μ modeling in difficult propagation conditions has been supported by recent works [34], [35], which this paper successfully applies to LF systems.

Lastly, a thorough performance review is made possible by the addition of performance measures including BER, channel capacity, and energy efficiency. This paper includes all three metrics, providing a more practical and balanced evaluation of LF system viability than some earlier publications that only examine one or two of them.

7. CONCLOUSIONS

In this work, we have discussed the LF as an attractive transceiver system from several different perspectives. We applied all principles of the transceiver system to LF which makes it very suitable for 5G networks. The BER and the Capacity of LF are provided and good improvement are shown compared with a previous channel models reported in literature. Also, we have compared our suggested model - of considering the LF as a good choice for the 5G system - with other previous works; there is a great match between what we proposed and the existing models in the literature. It is possible to significantly increase both spectral and energy efficiency by outfitting an LF with a large number of slots. Furthermore, we found that the power distribution of the LF system can be modeled by an α-μ distribution, which may be suitable for confined areas. However, in addition to considering the benefits of the LF as a large MIMO, further research is needed on a number of subjects, such as channel correlation, hardware implementations and impairments, interference control, and modulation, in addition to early test evaluation.

REFERENCES

[1] A. Tchinda, B. Shala, A. Lehmann, B. Ghita, D. Walker, U. Trick, "Energy-efficient placement of virtual network functions in a wireless mesh network," *IEEE Access*, vol. 12, pp. 64807–64822, 2024, doi: 10.1109/ACCESS.2024.3394907.

[2] A. Issa, N. Hakem, N. Kandil, "Combining leak feeder cable and antenna to support mobile network in underground mine environment," IEEE International Symposium on Antennas and Propagation and North American Radio Science Meeting, 2020, doi: 10.1109/IEEECONF35879.2020.9330109.

[3] H. Farahneh, X. Fernando, ''The leaky feeder, a reliable medium for vehicle to infrastructure communications,'' *Applied System Innovation*, vol. 2, no. 4, 2019, doi: 10.3390/asi2040036.

[4] O. Elalaouy, M. El Ghzaoui, J. Foshi, '' A low profile four-port MIMO array antenna with defected ground structure for 5G IoT applications,'' *Jordan Journal of Electrical Engineering*, vol. 9, no. 4, 2023, doi: 10.5455/jjee.204-1673904693.

[5] K. Zhang, G. Zheng, H. Wang, C. Zhang, X. Yu, '' Channel model and performance analysis for MIMO systems with single leaky coaxial cable in tunnel scenarios,'' *Sensors*, vol. 22, no. 15, 2022, doi: 10.3390/s22155776.

[6] J. Chen, Q. Chu, "Mixed metal decoupling structure for 5G MIMO base station antenna array," 16th UK-Europe-China Workshop on Millimetre Waves and Terahertz Technologies, 2023, doi: 10.1109/UCMMT58022.2023.10418946.

[7] Z. Siddiqui, M. Sonkki, M. Tuhkala, S. Myllymaki, ''Leaky coaxial cable with enhanced radiation performance for indoor communication systems, '' 16th International Symposium on Wireless Communication Systems, 2019, doi: 10.1109/ISWCS.2019.8877317.

[8] J. Guo, Y. Liu, X. Han, D. Li, "Research on attenuation model of the communication leaky coaxial cable," IEEE International Conference on Communication Technology, 2017, doi: 10.1109/ICCT.2017.8359823.

[9] M. Atmadja, F. Arinie, H. Kristiana, A. Indrianto, "Leaky feeder as a VoIP transmission medium," *West Science Interdisciplinary Studies*, vol. 2, pp 2020-2028, 2024, doi: 10.58812/wsis.v2i10.1339.

[10] D. Kassam, J. Castanheira, "A review on cell-free massive mimo systems," *Electronics*, vol. 12, no. 4, 2023, doi: 10.3390/electronics12041001.

[11] F. Larsson, O. Edfors, T. Marzetta, "Massive MIMO for next generation wireless systems," *IEEE Communications Magazine*, vol. 52, no. 2, pp. 186–195, 2014, doi: 10.1109/MCOM.2014.6736761.

[12] X. Zhong, X. Yin, X. Li, "Extension of ITU IMTadvanced channel models for elevation domains and line-of sight scenarios," 78th IEEE Vehicular Technology Conference, 2013, doi: 10.1109/VTCFall.2013.6692203.

[13] A. Maharani, H. Hudiono, "Optimization of 5 GHz wi-fi network performance using leaky feeder cables in building infrastructure," *West Science Interdisciplinary Studies*, vol. 2, p. 1717–1725, 2024, doi: 10.58812/wsis.v2i09.1263.

[14] Y. Liu, B. Ai, J. Zhang, "Downlink spectral efficiency of massive mimo systems with mutual coupling," *Electronics*, vol. 12, no. 6, 2023, doi: 10.3390/electronics12061364.

[15] M. Soleymani, I. Santamaria, A. Sezgin, E. Jorswieck, "Maximizing spectral and energy efficiency in multi-user mimo ofdm systems with ris and hardware impairment," *arXiv preprint*, 2024, doi: arXiv:2401.11921, 2024.

[16] J. Zhu, Y. Dong, J. Zhang, F. Guo, Q. Lu, L. Bin, J. Wu, ''Review on tunnel communication technology,'' *Sustainability*, vol. 14, no. 18, p. 11451, 2022, doi: 10.3390/su141811451.

[17] B. Saoud, I. Shayea, "Performance evaluation of MIMO-OFDM system in wireless network," International Conference on Wireless Networks and Mobile Communications, 2023, doi: 10.1109/WINCOM59760.2023.10322997.

[18] R. Othman, T. Alqaradaghi, A. Ameen, ''Efficient RMS delay spread-based physical layer abstraction modelling for enhanced 5G new radio performance evaluation,'' *Jordan Journal of Electrical Engineering*, vol. 10, no. 4, pp. 674–686, 2024, doi: 10.5455/jjee.204-1710439524.

[19] H. Abeida, '' Data-aided SNR estimation in time-variant rayleigh fading channels'', *IEEE Transactions on Signal Processing*, vol. 58, no. 11, pp. 5496-5507, 2010, doi: 10.1109/TSP.2010.2063429.

[20] S. Debnath, S. Ahmed, S. Alam, ''Analysis of filtered multicarrier modulation techniques using different windows for 5G and beyond wireless systems,'' *Wireless Communications and Mobile Computing*, vol. 2024, p. 9428292, 2024, doi: 10.1155/2024/9428292.

[21] J. Bai, J. He, Y. Chen, Y. Shen, X. Jiang, ''On achievable covert communication performance under CSI estimation error and feedback delay,'' 2024, doi: arXiv preprint arXiv:2404.05983.

[22] T. Marzetta, "Multi-cellular wireless with base stations employing unlimited numbers of antennas," *IEEE Transactions on Wireless Communications*, vol. 9, no. 11, pp. 3590-3600, 2010, doi: 10.1109/TWC.2010.092810.091092.

[23] P. Matthaiou, M. MacKay, J. Nossek, "On the condition number distribution of complex Wishart matrices," *IEEE Transactions on Communications*, vol. 58, no. 6, pp. 1705–1717, 2010, doi: 10.1109/TCOMM.2010.06.090328.

[24] Li, Shuang, "Matched filtering in massive MU-MIMO systems," Open Access The Herenga Waka-Victoria University of Wellington, PhD Thesis, 2020, doi: 10.26686/wgtn.17144072.

[25] S. Liang, C. Ho, "Block-iterative generalized decision feedback equalizers BI-GDFE for large MIMO systems: Algorithm design and asymptotic performance analysis," *IEEE Transactions on Signal Processing*, vol. 54, no. 6, pp. 2035–2048, 2006, doi: 10.1109/TSP.2006.873485.

[26] Z. Abbasi, H. Mustafa, J. Baik, M. Adnan, W. Awan, H. Song, "Hybrid wideband beamforming for sum spectral efficiency maximization in millimeter-wave relay-assisted multiuser MIMO cognitive radio networks," *Mathematics*, vol. 11, no. 24, 2023, doi: 10.3390/math11244939.

[27] M. Gursoy, "On the capacity and energy efficiency of training-based transmissions over fading channels," *IEEE Transactions on Information Theory*, vol. 55, no. 10, pp. 4543–4567, 2009, doi: 10.1109/TIT.2009.2027544.

[28] A. Chandar, D. Tse, "Asynchronous capacity per unit cost," *IEEE Transactions on Information Theory*, vol. 59, no. 3, pp. 280–284, 2010, doi: 10.1109/TIT.2012.2236914.

[29] Y. Chen, S. Zhang, S. Xu, G. Li, "Fundamental tradeoffs on green wireless networks," *IEEE Communications Magazine*, vol. 49, no. 6, pp. 30–37, 2011. doi: 10.1109/MCOM.2011.5783982.

[30] *The MathWorks, Inc, MATLAB-The Language of Technical Computing*, 2020, https://www.mathworks.com.

[31] M. Yacoub, "The α-μ distribution: a physical fading model for the stacy distribution," *IEEE Transactions on Vehicular Technology*, vol. 56, no. 1, pp. 27-34, 2007, doi: 10.1109/TVT.2006.883753.

[32] Z. Zheng, G. Wang, H. Zhang, Yu, X, ''Channel model and performance analysis for MIMO systems with single leaky coaxial cable in tunnel scenarios,'' *Sensors*, vol. 22, no. 15, p. 5776, 2022, doi: 10.3390/s22155776.

[33] R. Chataut, R. Akl, "Massive MIMO systems for 5G and beyond networks overview: recent trends, challenges, and future research direction," *Sensors,* vol. 20, p. 2753, 2023, doi: 10.3390/s20102753.

[34] M. Yacoub, ''The α-μ distribution: A physical fading model for the Stacy distribution,'' *IEEE Transactions on Vehicular Technology*, vol. 56, no. 1, pp, 27–34, 2007, doi: 10.1109/TVT.2006.883753.

[35] J. Zhu, P. Hou, Y. Hou, S. Denno, M. Okada, ''A study for 2-D indoor localization using multiple leaky coaxial cables,'' Z*PSIPA Transactions on Signal and Information Processing*, vol. 9, no. e20, 2020, doi: 10.1017/ATSIP.2020.18.